# Potential-Induced Aggregation of Anionic Porphyrins at Liquid|Liquid Interfaces



doi: 10.1021/acs.langmuir.7b01422

# Potential-Induced Aggregation of Anionic Porphyrins at Liquid|Liquid Interfaces

Sho Yamamoto,[†] Hirohisa Nagatani*[,‡] and Hisanori Imura[‡]

[†] Division of Material Chemistry, Graduate School of Natural Science and Technology, Kanazawa University, Kakuma, Kanazawa 920-1192, Japan

[‡] Faculty of Chemistry, Institute of Science and Engineering, Kanazawa University, Kakuma, Kanazawa 920-1192, Japan

*To whom correspondence should be addressed: H. Nagatani

Tel: +81 76 264 5692; FAX: +81 76 264 6059; E-mail: nagatani@se.kanazawa-u.ac.jp

**ABSTRACT**

The adsorption and self-aggregation of anionic porphyrins were studied at the polarized water|1,2-dichloroethne (DCE) interface by polarization-modulation total internal reflection fluorescence (PM-TIRF) spectroscopy. 5,10,15,20-Tetrakis(4-sulfonatophenyl)porphyrin diacid ($H_4TPPS^{2-}$) and protoporphyrin IX ($H_2PP^{2-}$) exhibited high surface activities at the interface. The selective excitation of interfacial species in PM-TIRF measurements elucidated the potential-induced aggregation mechanism of the porphyrins. The J-aggregates of $H_4TPPS^{2-}$ were reversibly formed only at the water|DCE interface by applying appropriate potentials even when the porphyrins exist as monomers in the aqueous and organic solutions. In the $H_2PP^{2-}$ system, the slow aggregation process was found in the negative potential region. The spectral characteristics and signal phase of PM-TIRF indicated that the $H_2PP^{2-}$monomers were adsorbed with relatively standing orientation and the long axis of the J-aggregates was nearly in plane of the interface. $H_2PP^{2-}$ was also investigated at the biomimetic phospholipid-adsorbed water|DCE interface. The competitive adsorption of neutral glycerophospholipids effectively inhibited the potential-dependent adsorption and interfacial aggregation processes of $H_2PP^{2-}$. The results demonstrated that the aggregation state of charged species could reversibly be controlled at liquid|liquid interfaces as a function of externally applied potential.

Keywords: polarization-modulation total internal reflection fluorescence (PM-TIRF) spectroscopy; interface between two immiscible electrolyte solutions (ITIES); water-soluble porphyrin; self-aggregation; biomimetic phospholipid-adsorbed interface

## 1. INTRODUCTION

Charge transfer processes at an interface between two immiscible electrolyte solutions (ITIES) have been studied to understand mass-transfer mechanism and distribution equilibrium in separation sciences, nanomaterial formation, pharmacokinetic applications and so on. The transfer and partition of ionic species across ITIES are controlled as a function of the Galvani potential difference between two liquid phases.[1, 2] The interfacial adsorption process is often involved in the ion transfer reaction. Direct characterization of molecules adsorbed at ITIES is essential to elucidate the heterogeneous reaction mechanism. The reactivity and characterization of interfacial species are generally evaluated by either electrochemical or spectrometric approach.[3-5] Some specific features of interfacial species have been reported in terms of molecular assembly and solvation by means of surface-sensitive spectroscopy.[6-8] It is known that various surface-active species tend to form their self-aggregates easily at liquid|liquid interfaces in comparison with homogeneous solution systems.[9-11] It is however still difficult to characterize the interfacial species with high sensitivity and selectivity at such an interface buried in proximal two bulk solution phases.

Potential-modulation inducing periodic modulation of spectroscopic signals from charged species is one of the most useful techniques to improve the sensitivity for the charge transfer reaction at ITIES.[12] Indeed, potential-modulated fluorescence (PMF) spectroscopy provides us mechanistic insights of the potential-dependent charge transfer phenomena. The interfacial reactions of a variety of charged fluorescent species and their associates have been investigated by PMF spectroscopy.[13-18] The characterization of the interfacial species has been achieved for *meso*-tetrakis(*N*-methylpyridyl)porphyrin ($H_2TMPyP^{4+}$) and *meso*-tetrakis(4-sulfonatophenyl)porphyrin ($H_2TPPS^{4-}$) systems,[19] where the PMF results demonstrated the specific solvation structure of interfacial species. Although the detailed PMF studies elucidate the dynamic behavior of monomeric ions such as ion transfer and adsorption processes, the characterization of interfacial species is available within limited experimental conditions since a

large change in molecular emission property caused by self-aggregation and ion-association complicates the signal analysis.[20, 21]

Recently, we have developed polarization-modulation total internal reflection fluorescence (PM-TIRF) spectroscopy and applied to study the potential-dependent adsorption behavior of *meso*-substituted water-soluble porphyrins at the water|1,2-dichloroethane (DCE) interface.[22] In the PM-TIRF experiments, the fluorescence signal from the interfacial region is analyzed as a function of periodic modulation of linear-polarizations of an incident excitation beam. PM-TIRF spectroscopy can effectively extract the fluorescence responses of molecules oriented at the interface because of no PM-TIRF signal arising from randomly oriented species such as bulk solution species. The wavelength-dependence of PM-TIRF signal corresponds to a pure fluorescence spectrum of oriented species, which allows us to characterize interfacial species with high selectivity. The PM-TIRF analysis of the cationic $H_2TMPyP^{4+}$ oriented at the water|DCE interface has demonstrated that $H_2TMPyP^{4+}$ was adsorbed with a modification of the hydration structure depending on $\Delta_o^w\phi$.

In the present study, the self-aggregation features of anionic water-soluble porphyrins, 5,10,15,20-tetrakis(4-sulfonatophenyl)porphyrin diacid ($H_4TPPS^{2-}$) and protoporphyrin IX ($H_2PP^{2-}$), were investigated at the polarized water|DCE interface by PM-TIRF spectroscopy. The TPPS species preferably form self-aggregates in solutions,[23-26] emulsions,[27, 28] and at liquid interfaces,[29-31] where the aggregation is significantly affected by the protonation of pyrrole nitrogens in a porphyrin ring, counter ions, electric field and so on. The effect of Galvani potential difference on the aggregation is, however, not elucidated at liquid|liquid interface. Protoporphyrin IX ($H_2PP^{2-}$) is one of the most important natural porphyrins and it has attracted much attention in supramolecular science, nanostructure assembly, energy and electron transfer systems on surfaces and at interfaces.[32, 33] The binding behavior of $H_2PP^{2-}$ to cell membranes is also crucial to understand its role as the photosensitizer in the photodynamic therapy because $H_2PP^{2-}$ is endogenously generated and selectively accumulated in cancer cells.[34, 35] While $H_2PP^{2-}$ has been examined at the water|DCE interface by PMF spectroscopy,[19] the interfacial mechanism

of $H_2PP^{2-}$ was hardly elucidated in detail because of its high surface-activity which weakened potential-modulated signals. By using PM-TIRF spectroscopy, the interfacial aggregation mechanisms of $H_4TPPS^{2-}$ and $H_2PP^{2-}$ were successfully analyzed as a function of Galvani potential difference. Furthermore, we investigated the adsorption behavior of $H_2PP^{2-}$ at the phospholipid-adsorbed water|DCE interface in order to evaluate its binding characteristics on cell membranes.

## 2. EXPERIMENTAL SECTION

**2.1. Reagents.** 5,10,15,20-Tetrakis(4-sulfonatophenyl)porphyrin ($H_2TPPS^{4-}$) disulfuric acid tetrahydrate (Dojindo Laboratories) and protoporphyrin IX ($H_2PP^{2-}$) disodium salt (TCI, GR) were used as received. The compositions of the electrochemical cell are represented in **Figure 1**. The pH of the aqueous phase was controlled by the addition of $5.0 \times 10^{-3}$ mol dm$^{-3}$ $H_2SO_4$ in **Cell I** and $1.0 \times 10^{-3}$ mol dm$^{-3}$ $LiH_2PO_4$/LiOH buffer in **Cell II**. The free base $H_2TPPS^{4-}$ ($pK_{a1}$ = 4.86, $pK_{a2}$ = 4.96[36, 37]) initially added into the aqueous phase exists as the diacid form ($H_4TPPS^{2-}$) in **Cell I** (**Figure S1,** Supporting Information). The supporting electrolytes were $1.0 \times 10^{-2}$ mol dm$^{-3}$ $Li_2SO_4$ (**Cell I**) or LiCl (**Cell II**) for the aqueous phase and $5.0 \times 10^{-3}$ mol dm$^{-3}$ bis(triphenylphosphoranylidene)ammonium tetrakis(pentafluorophenyl)borate (BTPPATPFB) for the organic phase, respectively. BTPPATPFB was prepared by metathesis of bis(triphenylphosphoranylidene)ammonium chloride (BTPPACl) (Aldrich, >97%) and lithium tetrakis(pentafluorophenyl)borate ethyl ether complex (TCI, ≥70%).[38] The aqueous solutions were prepared with purified water by a Milli-Q system (Millipore, Direct-Q3UV). 1,2-Dichloroethane (DCE) of HPLC grade (Nacalai Tesque, >99.7%) and purified water saturated with each other were used as solvents in the electrochemical measurements. A neutral glycerophospholipid, 1,2-dimyristoyl-*sn*-glycero-3-phosphocholine (DMPC) (TCI, ≥97%) was initially dissolved in chloroform at $1.0 \times 10^{-3}$ mol dm$^{-3}$ and then added to the DCE phase for the biomimetic interface (**Cell II**). All other reagents were of analytical grade or higher.

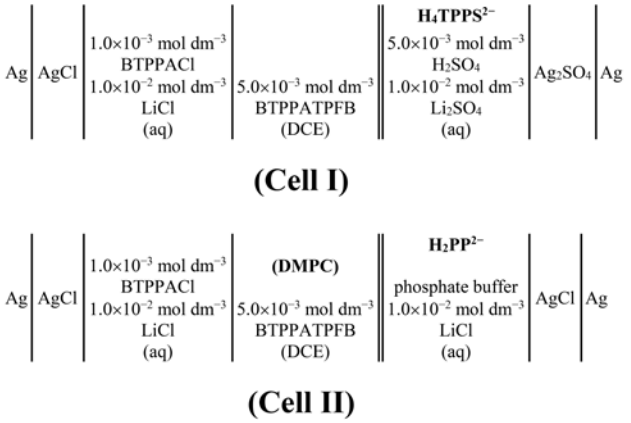


**Figure 1**. Schematic representation of the electrochemical cells.

**2.2. Spectroelectrochemical Setup.** The spectroelectrochemical cell was analogous to one reported previously.[22] The water|DCE interface with a geometrical area of 0.50 $cm^2$ was polarized by a four-electrode potentiostat (Hokuto Denko, HA-1010mM1A). Platinum wires were used as counter electrodes in both aqueous and organic phases. The Luggin capillaries were provided for the reference electrodes (Ag/AgCl or $Ag/Ag_2SO_4$) in both phases. The Galvani potential difference ( $\Delta_o^w\phi \equiv \phi^w - \phi^o$ ) was estimated by taking the formal transfer potential ( $\Delta_o^w\phi^{o\prime}$ ) of tetramethylammonium ions as 0.160 V. [39]

In PM-TIRF measurement, the water|DCE interface was illuminated in total internal reflection (TIR) mode from organic phase by a cw laser diode at 404 nm (Coherent, CUBE 405-50C) or 488 nm (Coherent, OBIS 488LS-60). The angle of incidence to the interface was set as ca. 75°. The laser radiation was attenuated to 25 mW in order to avoid the photobleaching of porphyrins. The fluorescence signal from the interfacial region was measured perpendicularly to the interface by an optical fiber and a monochromator equipped with a photomultiplier tube (Shimadzu, SPG-120S). The linear polarization of incident excitation beam was periodically modulated between p- (parallel to the plane of incidence) and s-polarizations (perpendicular to the plane of incidence) at 13 Hz by a liquid crystal retarder (LCR) (Thorlabs, LCC1111T-A, LCC25/TC200). The polarization modulation efficiency ($P_m$) of LCR was defined as the fraction of the p- or s-polarized component in the modulated-incident beam and measured through a Glan Thompson

prism (Sigma Koki, GTPC-10-33SN). The $P_m$ values were obtained as 0.95 at 404 nm and 0.97 at 488 nm, respectively, indicating that 5 and 3% of the s-polarized component remain in the p-polarized incident beam or *vice versa*.[22] The polarization-modulated fluorescence signal was analyzed by a digital lock-in amplifier (NF, LI5640) as a function of periodic modulation between the p- and s-polarized incident beams. All experiments were carried out in a thermostated room at 298 ± 2 K.

**2.3. Interfacial tension measurement.** The electrocapillary curves at 298 ± 2 K were measured at the polarized water|DCE interface by quasi-elastic laser scattering (QELS). A cylindrical glass cell with a geometrical interfacial area of 15.9 $cm^2$ was used in the interfacial tension measurements with the same cell composition displayed in **Figure 1**. The laser light beam passing through the interface perpendicularly was a cw laser at 660 nm (Coherent, CUBE 660-60C). The diffraction grating with a line spacing of 0.320 mm was placed after the water|DCE interface. The optical beat of third-order diffraction spot was detected by a Si photodiode (Hamamatsu Photonics, S1133-01) with a wide bandwidth amplifier (Melles Griot, 13AMP005). The power spectra of the diffraction spot were obtained by using a fast-Fourier transform analyzer (Stanford Research Systems, SR770). The interfacial tension ($\gamma_i$) was calculated from the frequency of maximum intensity associated with the mean frequency of the capillary waves. Further detail of optical setup and analytical procedure of QELS were described elsewhere.[40, 41]

## 3. RESULTS AND DISCUSSION

**3.1. Electrochemical Responses of Anionic Porphyrins at the Water|DCE Interface.** Cyclic voltammograms (CVs) and ac voltammograms measured for $H_4TPPS^{2-}$ at pH 2.1 (**Cell I**) and $H_2PP^{2-}$ at pH 7.3 (**Cell II**) are displayed in **Figure 2**. The distinct admittance responses were observed for $H_4TPPS^{2-}$ around −0.25 V and a peak separation of ca. 16 mV in CVs corresponds to a diffusion-controlled transfer process of tetravalent ions (**Figure 2a**). These voltammetric responses thus associate with the ion transfer of $H_2TPPS^{4-}$ across the interface. The ion transfer mechanism of $H_4TPPS^{2-}$ has been reported in detail at the water|nitrobenzene interface, where

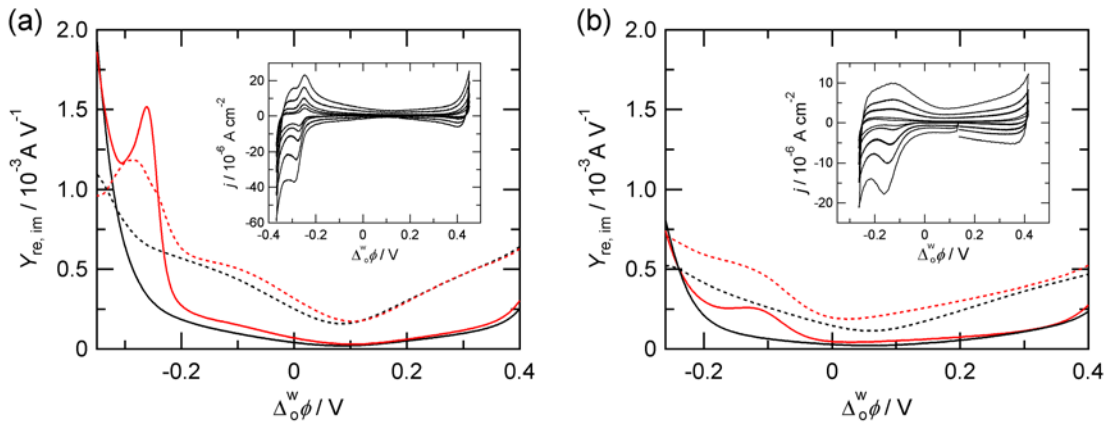


**Figure 2.** Ac voltammograms measured for **(a)** $H_4TPPS^{2-}$ at pH 2.1 and **(b)** $H_2PP^{2-}$ at pH 7.3. The red and black lines depict ac voltammograms in the presence and absence of the porphyrins. The solid and dashed lines denote the real and imaginary components of admittance. The potential sweep rate was 5 mV $s^{-1}$. The potential modulation was 10 mV at 7 Hz. **(Inset)** CVs measured at 10, 20, 50, 100 and 200 mV $s^{-1}$. The concentrations of $H_4TPPS^{2-}$ and $H_2PP^{2-}$ in the aqueous phase were $2.0 \times 10^{-5}$ mol $dm^{-3}$ and $1.0 \times 10^{-4}$ mol $dm^{-3}$, respectively.

the deprotonated free base ($H_2TPPS^{4-}$) was dominant transferred species even under acidic conditions because of enhanced hydrophilicity of $H_4TPPS^{2-}$.[42] A 50 mV negative shift of the transfer potential of $H_2TPPS^{4-}$ (cf. $\Delta^{w}_{o}\phi^{\circ'}_{H_2TPPS^{4-}}$ = –0.20 V[19, 22]) results from the protonation equilibrium in aqueous solution. In the $H_2PP^{2-}$ system, a pair of positive and negative current peaks was observed at –0.13 V but the broad positive peaks were relatively small (**Figure 2b**, inset). These voltammetric features should be attributed to the ion transfer process of $H_2PP^{2-}$ accompanied by the interfacial adsorption since the negative peak currents at –0.13 V were linearly proportional to the sweep rate in agreement with the previous report.[19] The formal transfer potential of $H_2PP^{2-}$ was evaluated at $\Delta^{w}_{o}\phi^{\circ'}_{H_2PP^{2-}}$ = –0.13 V from ac voltammograms.

The adsorption of the porphyrins at the water|DCE interface can be confirmed by small increments of the admittance. In **Figure 2**, the real ($Y_{re}$) and imaginary ($Y_{im}$) components of the

admittance increase prior to the transfer potential in both systems, indicating the specific adsorption of the anionic porphyrins at the interface. The adsorption responses of $H_4TPPS^{2-}$ were obtained at $\Delta_o^w\phi$ < 0.10 V, while those of $H_2PP^{2-}$ appeared within the whole potential window. Indeed, the electrocapillary curves in **Figure S2** (Supporting Information) showed that the $\gamma_i$ values were decreased at $\Delta_o^w\phi$ < 0 V in the presence of $H_4TPPS^{2-}$. The interfacial tension lowering by adding $H_2PP^{2-}$ was also measured over the potential window. These results could indicate that adsorption process of $H_2PP^{2-}$ is less potential-dependent in comparison with $H_4TPPS^{2-}$.

**3.2. PM-TIRF Analysis of Adsorption and Aggregation of Porphyrins at the Water|DCE Interface.** The PM-TIRF spectroscopy was employed to elucidate the potential-dependent adsorption behavior of the porphyrin at the water|DCE interface. The PM-TIRF signal ($\Delta F^{p\text{-}s}$) is defined as

$$\Delta F^{p\text{-}s} = F_m^p - F_m^s \quad (1)$$

where $F_m^p$ and $F_m^s$ are the fluorescence intensities measured with p- and s-polarized excitation modes, respectively. In PM-TIRF spectroscopy, the fluorescence signal arising from bulk solution species with random orientation is effectively cancelled out. The wavelength-dependence of PM-TIRF signal, i.e. PM-TIRF spectrum, was measured at given potentials. PM-TIRF spectrum corresponds to the fluorescence spectrum of interfacial species oriented at the interface. The positive and negative $\Delta F^{p\text{-}s}$ indicate relatively standing and lying orientations of the porphyrin ring with respect to the interface since the porphyrin molecule contains two perpendicular transition dipole moments within the porphyrin plane.[43, 44] It should be noted that a zero $\Delta F^{p\text{-}s}$ relates to random or specific orientation at the magic angle (54.7°).[22]

**Figure 3** shows the PM-TIRF spectra measured for $H_4TPPS^{2-}$ at pH 2.2 under potentiostatic control. The incident laser beams of 404 nm and 488 nm were employed for the excitation of the

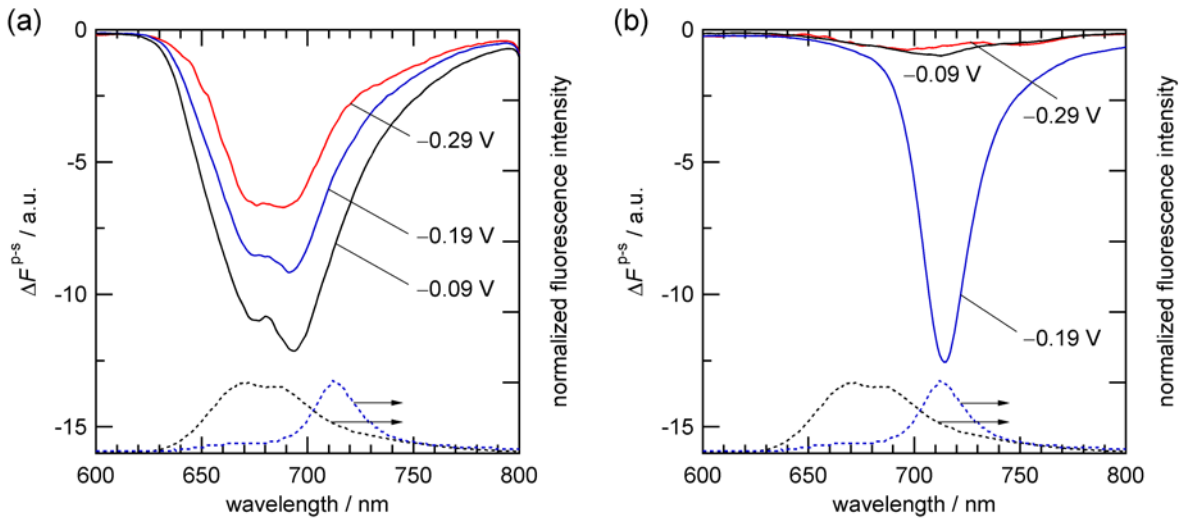


**Figure 3.** PM-TIRF spectra for $H_4TPPS^{2-}$ at the water|DCE interface under the excitation at **(a)** 404 nm and **(b)** 488 nm. The pH of the aqueous phase was pH 2.2. The blue and black dotted lines refer to the normalized fluorescence spectra of J-aggregates at pH 1.3 and monomers at pH 2.3 in the aqueous solutions under the excitation at 488 nm.

monomer and aggregate species of $H_4TPPS^{2-}$, respectively. The formation of J-aggregates with red-shifted emission bands at the interface were clearly observed depending on $\Delta_o^w\phi$. It is known that $H_4TPPS^{2-}$ tends to form J-aggregate under lower pH conditions through the coulomb interaction between its diprotonated porphyrin ring and anionic sulfonatophenyl groups. The J-aggregates retain the structure in a suitable slipped face-to-face stacking.[45, 46] The monomeric $H_4TPPS^{2-}$ shows the Soret and Q bands around 434 nm and 645 nm in aqueous solution, while the J-aggregates of $H_4TPPS^{2-}$ exhibit sharp and intense absorption bands around 491 nm and 707 nm (**Figure S1a**, Supporting Information).[47-49] In the PM-TIRF measurement, the $\Delta F^{p\text{-}s}$ signals from the interfacial species should be associated with the orientations of the porphyrin ring of monomers or the long axis of aggregates.[50, 51] The fluorescence maximum wavelengths of the PM-TIRF spectra are summarized in **Table 1.** In **Figure 3a**, the PM-TIRF spectra with a negative sign ($\Delta F^{p\text{-}s} < 0$) exhibited similar features to the fluorescence spectra of the diacid form in aqueous solution, indicating that the $H_4TPPS^{2-}$ monomers were adsorbed with relatively

lying orientation ($54.7° < \theta \leq 90°$) and its adsorption state was almost consistent with that in the bulk aqueous phase. The non-zero $\Delta F^{\text{p-s}}$ associated with the adsorption of $H_4TPPS^{2-}$ was also observed at −0.29 V, which is 0.04 V more negative potential than that of the ion transfer. The results show that the $H_4TPPS^{2-}$ monomers accumulate at the aqueous side of the interface. In addition, the interfacial adsorption of the free base, $H_2TPPS^{4-}$, was not found under the present experimental conditions.

**Table 1. Fluorescence maximum wavelengths of the porphyrins at the water|DCE interface and in solutions.**

| | TPPS system | | | PP system | | |
|---|---|---|---|---|---|---|
| | $\Delta^{\text{w}}_{\text{o}}\phi$ / V | $\lambda^{404}_{\text{em,max}}$ / nm[b] | $\lambda^{488}_{\text{em,max}}$ / nm[b] | $\Delta^{\text{w}}_{\text{o}}\phi$ / V | $\lambda^{404}_{\text{em,max}}$ / nm[b] | $R_{\text{F}}$[c] |
| interface (PM-TIRF)[a] | −0.09 | 676(−), 693(−) | 713(−) | 0.31 | 636(+), 702(+) | 4.8 |
| | −0.19 | 676(−), 691(−) | 714(−) | −0.11 | 636(+), 693(−) | |
| | −0.29 | 676(−), 688(−) | 697(−) | −0.20 | 640(−), 698(−) | 1.2 |
| aqueous phase[d] | | (pH 1.3) 671, 684 | 713 | | (pH 7.3) 620, 684 | 2.8 |
| | | (pH 2.3) 671, 684 | 671, 684 | | | |
| organic phase[d] | | 651, 715 | 651, 715 | | 633, 698 | 2.9 |

[a]The PM-TIRF spectra were taken at pH 2.2 for TPPS and pH 7.3 for PP systems. The parenthetic signs (+) and (−) denote the positive and negative PM-TIRF peaks, respectively. [b] $\lambda^{404}_{\text{em,max}}$ and $\lambda^{488}_{\text{em,max}}$ denote the PM-TIRF maxima under the excitation at 404 nm and 488 nm, respectively. [c]The peak intensity ratio of the first and second fluorescence peaks. [d]The fluorescence maxima measured for the aqueous and organic solutions (cf. **Figures S1** and **S3**, Supporting Information).

Under the excitation at 488 nm, the selective detection of J-aggregates of $H_4TPPS^{2-}$ was achieved with negligible interference from the monomer species. As seen in **Figure 3b**, the intensity of negative PM-TIRF signals was highly dependent on $\Delta^{\text{w}}_{\text{o}}\phi$ and a maximum wavelength of 714 nm clearly indicates the formation of the J-aggregates at the interface. The negative $\Delta F^{\text{p-s}}$ also suggests that the long axis of the J-aggregates was lying nearly parallel to

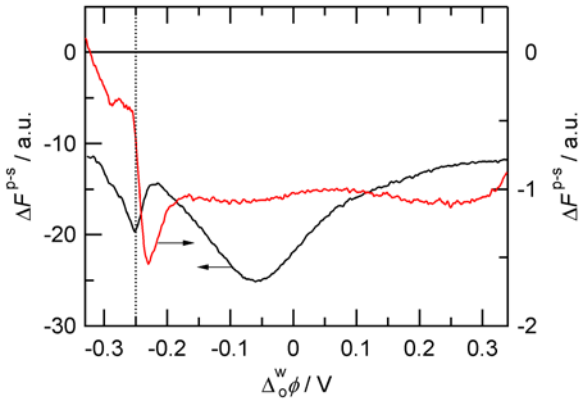


**Figure 4.** Typical potential dependence of PM-TIRF responses ($\Delta F^{p\text{-}s}$) for $H_4TPPS^{2-}$ at the water|DCE interface. The excitation and detection wavelengths were 404 nm and 680 nm (black line, left axis) and 488 nm and 713 nm (red line, right axis), respectively. The potential sweep rate was 1 mV $s^{-1}$. The vertical dotted line depicts the transfer potential at pH 2.2, i.e., $\Delta_o^w\phi$ = –0.25 V. The concentration of $H_2TPPS^{4-}$ in the aqueous phase was 2.0 × $10^{-5}$ mol $dm^{-3}$.

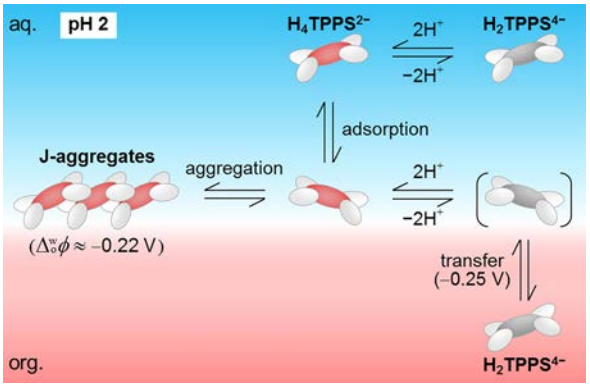


**Figure 5.** Schematic representation of the aggregation and transfer of $H_4TPPS^{2-}$ at the polarized water|DCE interface.

the interface. The PM-TIRF signals of $H_4TPPS^{2-}$ monomer and its aggregates were recorded respectively at 680 nm and 713 nm in the quasi-equilibrium condition with a potential sweep rate of 1 mV $s^{-1}$ (**Figure 4**). The potential dependence of $\Delta F^{p\text{-}s}$ indicates that the J-aggregation takes place at less negative potentials than that of the transfer (see also **Figures S4**, Supporting

Information). The negative $\Delta F^{p\text{-}s}$ magnitude of the monomer maximized around –0.07 V was decreased simultaneously with increasing negative $\Delta F^{p\text{-}s}$ signals attributable to the aggregation at –0.25 V < $\Delta_o^w\phi$ ≤ –0.15 V. At more negative potential, the magnitude of $\Delta F^{p\text{-}s}$ at 713 nm was reduced eventually to almost zero. It is noteworthy that the conventional TIR fluorescence spectra indicate that the bulk aqueous and organic solution species were monomeric $H_4TPPS^{2-}$ and $H_2TPPS^{4-}$, respectively (**Figure S5**, Supporting Information). Therefore, the J-aggregates of $H_4TPPS^{2-}$ were formed only at the aqueous side of the interface (**Figure 5**). The J-aggregate were dissociated through the transfer of monomer species and simultaneous interfacial concentration lowering. Although the free base from, $H_2TPPS^{4-}$, exists in very low abundance under acidic conditions, $H_2TPPS^{4-}$ should favorably be transferred at negative potentials in comparison with the diacid species, $H_4TPPS^{2-}$ which is more hydrophilic but the lower net charge.[42]

The PM-TIRF spectra measured for $H_2PP^{2-}$ showed complicated spectral features depending on $\Delta_o^w\phi$ under neutral pH conditions (**Figure 6**), where the further protonation of the free base is negligible. The PM-TIRF experiments for $H_2PP^{2-}$ were carried out under the excitation at 404 nm. The fluorescence maximum wavelengths and peak intensity ratios of the first and second peaks ($R_F$) of PM-TIRF spectra are summarized in **Table 1**. At positive potentials, the PM-TIRF spectra exhibited the positive PM-TIRF signals ( $\Delta F^{p\text{-}s} > 0$), suggesting that the $H_2PP^{2-}$ monomers were adsorbed with standing orientation relative to the interface. The PM-TIRF maxima, 636 nm and 702 nm, observed at 0.31 V were consistent with fluorescence maxima of $H_2PP^{2-}$ in the organic phase at 633 nm and 698 nm. These spectral features suggest that $H_2PP^{2-}$ adsorbed at the interface has a solvation state similar to the bulk organic solution species, i.e., dehydration of the porphyrin fluorophore. Taking into account relatively standing orientations of $H_2PP^{2-}$ under positively polarized conditions, the less hydrophilic porphyrin moiety of $H_2PP^{2-}$ could penetrate into the organic side of the interface. In the negative potential region, the positive PM-TIRF responses at 636 nm were gradually weakened and then the negative PM-TIRF spectra

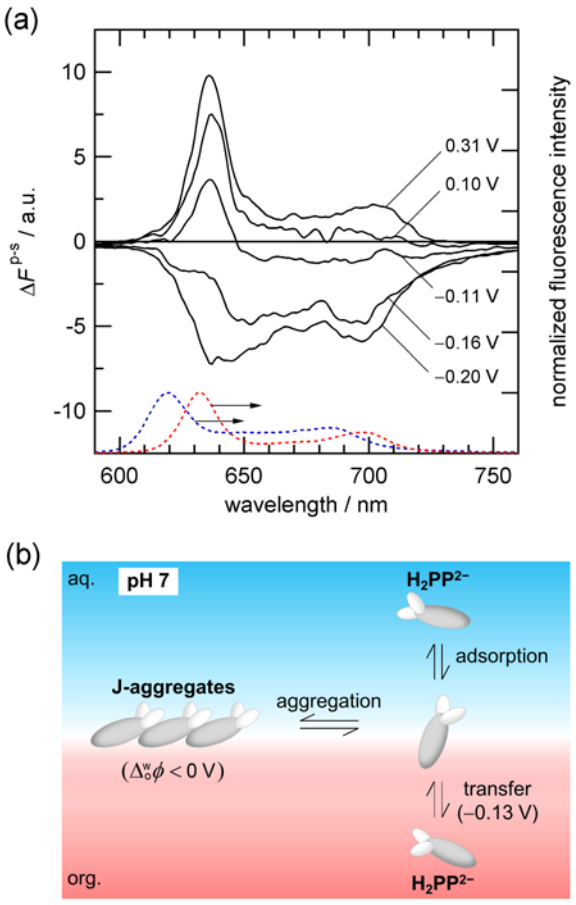


**Figure 6. (a)** Typical PM-TIRF spectra for $H_2PP^{2-}$ at the water|DCE interface. The blue and red dotted lines refer to the normalized fluorescence spectra measured in the aqueous and organic solutions. The concentration of $H_2PP^{2-}$ in the aqueous phase at pH 7.3 was $1.0 \times 10^{-4}$ mol $dm^{-3}$. The excitation wavelength was 404 nm. **(b)** Schematic representation of the aggregation and transfer of $H_2PP^{2-}$ at the water|DCE interface.

were obtained at $\Delta_o^w\phi < \Delta_o^w\phi^{\circ'}_{H_2PP^{2-}}$. As a result, a red-shifted broad peak around 640 nm appeared in the PM-TIRF spectrum at −0.20 V. The similar red-shift has been observed for Fe(III) protoporphyrin IX at the water|DCE interface by surface second harmonic generation (SSHG), where the spectral shift was interpreted by the aggregation and specific polarity in the interfacial region.[52] It has also been reported that the J-aggregation of $H_2PP^{2-}$ and its derivatives in solutions causes a significant decrease of fluorescence intensities with a small spectral shift in

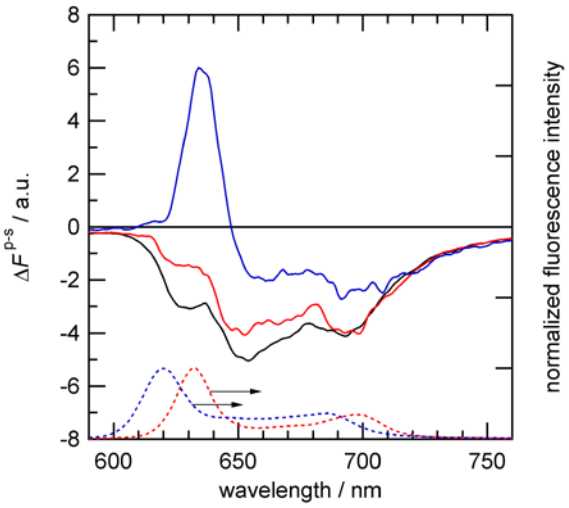


**Figure 7.** The dependence of PM-TIRF spectra at $\Delta^{w}_{o}\phi = -0.16$ V on the $H_2PP^{2-}$ concentration. The concentrations of $H_2PP^{2-}$ were $2.0 \times 10^{-5}$ (black), $1.0 \times 10^{-4}$ (red) and $5.0 \times 10^{-4}$ mol dm$^{-3}$ (blue). The blue and red dotted lines refer to normalized fluorescence spectra measured in the aqueous and organic solutions.

fluorescence spectrum.[53-55] In the same manner, the interfacial J-aggregation should be responsible for the relative red-shift in PM-TIRF spectra with $\Delta F^{p\text{-}s} < 0$. In the present pH condition, the J-aggregates consist of free base forms with the π-π interaction between porphyrin rings. **Figure 6b** illustrates the interfacial mechanism of $H_2PP^{2-}$. The J-aggregation occurs only at the negatively polarized interface, and the $H_2PP^{2-}$ monomers transfer at –0.13 V as described in Section 3.1. The J-aggregation of $H_2PP^{2-}$ was considerably slow process at the polarized water|DCE interface and it takes more than 20 minutes for the equilibrium (see **Figure S6**, Supporting Information). These specific interfacial behavior could be attributed to the high surface-activity and well-ordered molecular orientation of $H_2PP^{2-}$ at the water|DCE interface.

The PM-TIRF results at various concentrations of $H_2PP^{2-}$ demonstrated that the potential-induced aggregation occurs even at dilute concentrations down to $2.0 \times 10^{-5}$ mol dm$^{-3}$ (**Figure S7**, Supporting Information). **Figure 7** shows the concentration dependence of PM-TIRF spectra measured at –0.16 V, where the spectral features were changed from the red-shifted spectrum of

the J-aggregates with $\Delta F^{\text{p-s}} < 0$ to the monomeric shape with $0 < \Delta F^{\text{p-s}}$ at higher concentrations. It is known that the aggregation of porphyrins was induced by increasing the bulk concentration.[55-57] The PM-TIRF spectrum at $5.0 \times 10^{-4}$ mol dm$^{-3}$, however, showed the sharp monomeric response with a positive sign at 636 nm (**Figure S8**, Supporting Information). The possible reason for the $H_2PP^{2-}$ monomer as the dominant interfacial species is the limited interfacial area available for the adsorption since an upstanding molecular orientation of monomeric $H_2PP^{2-}$ can reduce the occupied interfacial area per unit molecule in comparison with the aggregates flattened in the interfacial plane.

**3.3. Adsorption Behavior of $H_2PP^{2-}$ at a Biomimetic Interface.** The phospholipids with a high surface-activity are spontaneously adsorbed at liquid|liquid interfaces and their adsorption layers can be used as a model of biomembrane surface.[58-60] In this study, the neutral glycerophospholipid, DMPC, was added into the organic phase (**Cell II**). **Figure 8** shows the CVs and electrocapillary curves for $H_2PP^{2-}$ at the DMPC-adsorbed water|DCE interface. The current increase at 0.20 V $< \Delta_o^w\phi$ in the presence of $1.0 \times 10^{-5}$ mol dm$^{-3}$ DMPC is associated with the facilitated transfer of $Li^+$ ions by the DMPC layer formed at the interface.[61, 62] The voltammetric responses of $H_2PP^{2-}$ around $\Delta_o^w\phi^{o'}_{H_2PP^{2-}} = -0.13$ V were significantly decreased with increasing DMPC concentration and almost vanished at a concentration of $1.0 \times 10^{-5}$ mol dm$^{-3}$. The voltammetric results demonstrated that the DMPC layer effectively inhibited the adsorption and transfer processes of $H_2PP^{2-}$. The surface-activity of both $H_2PP^{2-}$ and DMPC manifested itself in the $\gamma_i$ lowering in the electrocapillary curves in **Figure 8b**. The adsorption of DMPC caused a remarkable decrease in $\gamma_i$ and the additional lowering effect was observed by the coexistence of $H_2PP^{2-}$ at $\Delta_o^w\phi < 0.2$ V. These results imply that $H_2PP^{2-}$ penetrates into the DMPC layer formed at the negatively polarized interface.

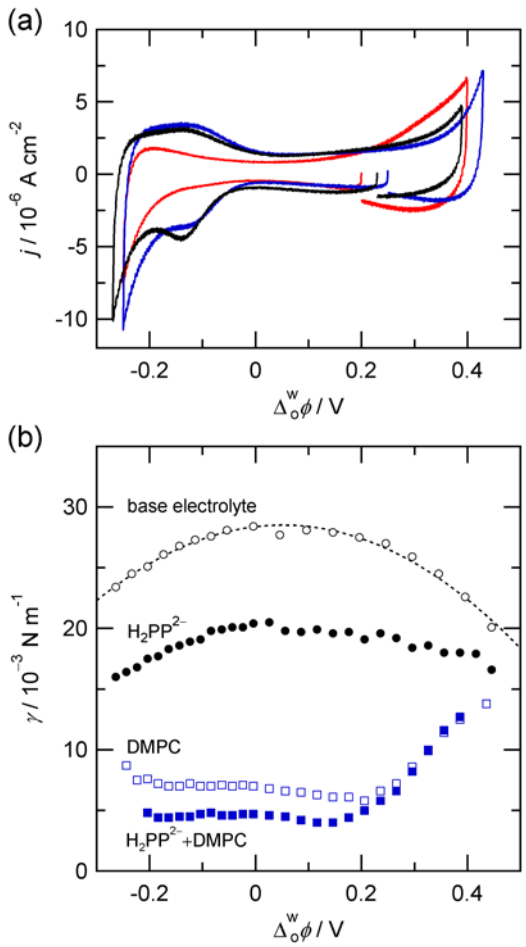


**Figure 8. (a)** CVs and **(b)** electrocapillary curves for $H_2PP^{2-}$ at the DMPC-adsorbed water|DCE interface. The concentration of $H_2PP^{2-}$ was $1.0 \times 10^{-4}$ mol dm$^{-3}$ and the aqueous phase was buffered at pH 7.2–7.3. **(a)** The concentrations of DMPC were 0 (black), $1.0 \times 10^{-6}$ (blue) and $1.0 \times 10^{-5}$ mol dm$^{-3}$ (red), respectively. The potential sweep rates were 50 mV s$^{-1}$. **(b)** The electrocapillary curves were measured in the presence of $H_2PP^{2-}$ (solid circle), $1.0 \times 10^{-5}$ mol dm$^{-3}$ DMPC (open square) and $H_2PP^{2-}$ + DMPC (solid square), respectively. The open circles depict the base electrolyte system.

The addition of DMPC also influenced the spectral shape and signal phase of PM-TIRF spectra measured at given potentials (**Figure 9).** At 0.31 V, the PM-TIRF response arising from $H_2PP^{2-}$ monomers was considerably weakened by the competitive adsorption with DMPC. This result agrees with a lack of additional $\gamma_i$ lowering at 0.2 V < $\Delta^{w}_{o}\phi$ in the presence of DMPC and

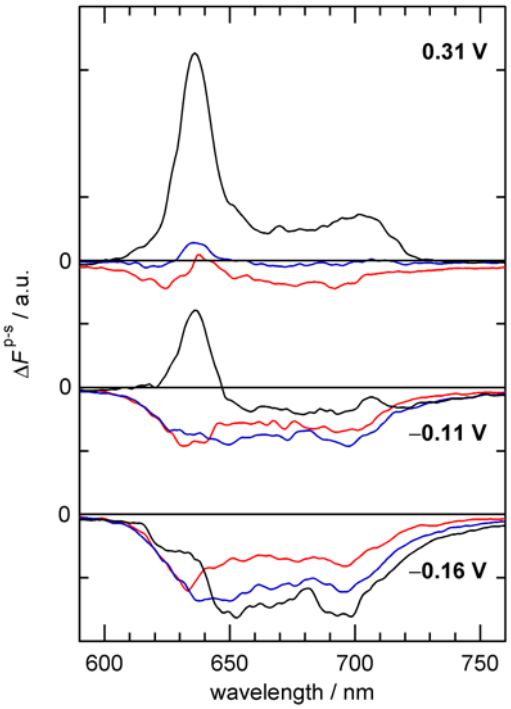


**Figure 9.** PM-TIRF spectra measured at the DMPC-adsorbed water|DCE interface. The concentrations of DMPC were 0 (black), $1.0 \times 10^{-6}$ (blue) and $1.0 \times 10^{-5}$ mol dm$^{-3}$ (red), respectively. The concentration of $H_2PP^{2-}$ was $1.0 \times 10^{-4}$ mol dm$^{-3}$.

$H_2PP^{2-}$ (**Figure 8b**). On the other hand, the PM-TIRF spectra at −0.16 V in the presence of $1.0 \times 10^{-5}$ mol dm$^{-3}$ DMPC showed the negative $\Delta F^{p\text{-}s}$ signals and the PM-TIRF maximum around 633 nm exhibited the similar spectral feature of the $H_2PP^{2-}$ monomer in the organic solution (cf. **Table 1**). At the negatively polarized interface, the $H_2PP^{2-}$ monomer penetrates into the DMPC layer and the spectral characteristics among neighboring alkyl chains should be analogous to those of the species in the organic phase.

## 4. CONCLUSIONS

The spectroelectrochemical analysis based on the PM-TIRF technique uncovered the potential-dependent adsorption and aggregation mechanism of anionic porphyrins at the polarized water|DCE interface. In the $H_4TPPS^{2-}$ system, the monomeric $H_4TPPS^{2-}$ and its J-aggregates

oriented at the interface could be measured separately by selecting the appropriate excitation wavelength. The selective detection of the interfacial species achieved in multi-wavelength excited PM-TIRF experiments is useful to elucidate the complicated heterogeneous mechanism, which is composed of charge transfer processes of plural surface-active species. The negative PM-TIRF signals exhibited the relatively flat orientation of the *meso*-substituted $H_4TPPS^{2-}$ monomer with four equivalent sulfonatophenyl groups, whereas the potential-induced J-aggregation of $H_4TPPS^{2-}$ proceeded only at the aqueous side of the interface. The slow aggregation process of $H_2PP^{2-}$ was found in the negative potential region. The molecular orientation of $H_2PP^{2-}$ was significantly affected by the J-aggregation at the interface, where the monomers were adsorbed with relatively standing orientation and the long axis of the J-aggregates was nearly in plane of the interface. At the phospholipid-adsorbed water|DCE interface, the competitive adsorption of DMPC effectively inhibited the adsorption and aggregation processes of $H_2PP^{2-}$. The adsorption state of $H_2PP^{2-}$ at the phospholipid-adsorbed interface was similar to the monomeric species in the organic phase. As the photoreactivity of porphyrins on cell membranes is drastically affected by the adsorption state, these findings could, for instance, contribute to the mechanistic analysis of the photodynamic therapy with endogenously generated $H_2PP^{2-}$ in cancer tissues. The present study demonstrated that the interfacial aggregation of charged species can reversibly be controlled as a function of externally applied potential and it will enable a potential-induced self-assembly of 2D supramolecular structure or nanomaterial formation at ITIES.

**Supporting Information:** UV-vis absorption and fluorescence spectra of the porphyrins in solutions, electrocapillary curves and PM-TIRF spectra measured under various conditions.

**ACKNOWLEDGMENTS**

This work was supported by Grants-in-Aid for Scientific Research (C) (no.16K05811) and Scientific Research (B) (no.25288064) from Japan Society for the Promotion of Science (JSPS).

We also acknowledge the Kanazawa University CHOZEN Project. S.Y. is grateful to the JSPS Research Fellowship for Young Scientists (no.17J02009).

**REFERENCES**

(1) Samec, Z., Electrochemistry at the Interface between Two Immiscible Electolyte Solutions. *Pure Appl. Chem.* **2004,** *76*, 2147-2180.

(2) Girault, H. H., Electrochemistry at Liquid-Liquid Interfaces. In *Electroanalytical Chemistry*, Bard, A. J.; Zoski, C. G., Eds. CRC Press: 2010; Vol. 23, pp 1-104.

(3) Volkov, A. G., *Liquid Interfaces in Chemical, Biological, and Pharmaceutical Application*. Marcel Dekker: New York, 2001.

(4) Watarai, H.; Teramae, N.; Sawada, S., *Interfacial Nanochemistry*. Kluwer Academic/Plenum Publishers: New York, 2005.

(5) Perera, J. M.; Stevens, G. W., Spectroscopic Studies of Molecular Interaction at the Liquid-Liquid Interface. *Anal. Bioanal. Chem.* **2009,** *395*, 1019-1032.

(6) Benjamin, I., Chemical Reactions and Solvation at Liquid Interfaces: A Microscopic Perspective. *Chem. Rev.* **1996,** *96*, 1449-1475.

(7) Benjamin, I., Reaction Dynamics at Liquid Interfaces. *Annu. Rev. Phys. Chem.* **2015,** *66*, 165-188.

(8) Nagatani, H., *In Situ* Spectroscopic Characterization of Porphyrins at Liquid Interfaces. In *Handbook of Porphyrin Science*, Kadish, K. M.; Smith, K. M.; Guilard, R., Eds. World Scientific Publishing Co.: Singapore, 2014; Vol. Volume 34: Harnessing Solar Energy pp 51-96.

(9) Watarai, H.; Adachi, K., Measuring the Optical Chirality of Molecular Aggregates at Liquid-Liquid Interfaces. *Anal. Bioanal. Chem.* **2009,** *395*, 1033-1046.

(10) Uchida, T.; Yamaguchi, A.; Ina, T.; Teramae, N., Observation of Molecular Association at Liquid/Liquid and Solid/Liquid Interfaces by Second Harmonic Generation Spectroscopy. *J. Phys. Chem. B* **2000,** *104*, 12093-12094.

(11) Pant, D.; Girault, H. H., Time-Resolved Total Internal Reflection Fluorescence Spectroscopy: Part I. Photophysics of Coumarin 343 at Liquid/Liquid Interface. *Phys. Chem. Chem. Phys.* **2005,** *7,* 3457-3463.

(12) Nagatani, H.; Sagara, T., Potential-Modulation Spectroscopy at Solid/Liquid and Liquid/Liquid Interfaces. *Anal. Sci.* **2007,** *23,* 1041-1048.

(13) Yoshimura, T.; Nagatani, H.; Osakai, T., Combined Use of Two Membrane-Potential-Sensitive Dyes for Determination of the Galvani Potential Difference across a Biomimetic Oil/Water Interface. *Anal. Bioanal. Chem.* **2014,** *406,* 3407-3414.

(14) Sakae, H.; Nagatani, H.; Morita, K.; Imura, H., Spectroelectrochemical Characterization of Dendrimer-Porphyrin Associates at Polarized Liquid|Liquid Interfaces. *Langmuir* **2014,** *30,* 937-945.

(15) Nagatani, H.; Sakamoto, T.; Torikai, T.; Sagara, T., Encapsulation of Anilinonaphthalenesulfonates in Carboxylate-Terminated PAMAM Dendrimer at the Polarized Water|1,2-Dichloroethane Interface. *Langmuir* **2010,** *26,* 17686-17694.

(16) Osakai, T.; Yamada, H.; Nagatani, H.; Sagara, T., Potential-Dependent Adsorption of Amphoteric Rhodamine Dyes at the Oil/Water Interface as Studied by Potential-Modulated Fluorescence Spectroscopy. *J. Phys. Chem. C* **2007,** *111,* 9480-9487.

(17) Sakae, H.; Fujisawa, M.; Nagatani, H.; Imura, H., Molecular Association between Flavin Derivatives and Dendritic Polymers at the Water|1,2-Dichloroethane Interface. *J. Electroanal. Chem.* **2016,** *782,* 288-292.

(18) Nishi, N.; Izawa, K.; Yamamoto, M.; Kakiuchi, T., AC-Modulated Voltfluorometric Study of the Transient Adsorption of Rose Bengal Dianions in the Transfer across the 1,2-Dichloroethane|Water Interface. *J. Phys. Chem. B* **2001,** *105,* 8162-8169.

(19) Nagatani, H.; Ozeki, T.; Osakai, T., Direct Spectroelectrochemical Observation of Interfacial Species at the Polarized Water/1,2-Dichloroethane Interface by Ac Potential Modulation Technique. *J. Electroanal. Chem.* **2006,** *588,* 99-105.

(20) Nagatani, H.; Suzuki, S.; Fermín, D. J.; Girault, H. H.; Nakatani, K., Interfacial Behavior of Sulforhodamine 101 at the Polarized Water/1,2-Dichloroethane Interface Studied by Spectroelectrochemical Techniques. *Anal. Bioanal. Chem.* **2006,** *386*, 633-638.

(21) Nakatani, K.; Nagatani, H.; Fermín, D. J.; Girault, H. H., Transfer and Adsorption of 1-Pyrene Sulfonate at the Water|1,2-Dichloroethane Interface Studied by Potential Modulated Fluorescence Spectroscopy. *J. Electroanal. Chem.* **2002,** *518*, 1-5.

(22) Yamamoto, S.; Nagatani, H.; Morita, K.; Imura, H., Potential-Dependent Adsorption and Orientation of *meso*-Substituted Porphyrins at Liquid|Liquid Interfaces Studied by Polarization-Modulation Total Internal Reflection Fluorescence Spectroscopy. *J. Phys. Chem. C* **2016,** *120*, 7248-7255.

(23) Gandini, S. C. M.; Gelamo, E. L.; Itri, R.; Tabak, M., Small Angle X-ray Scattering Study of *meso*-Tetrakis (4-Sulfonatophenyl) Porphyrin in Aqueous Solution: A Self-Aggregation Model. *Biophys. J.* **2003,** *85*, 1259-1268.

(24) Choi, M. Y.; Pollard, J. A.; Webb, M. A.; McHale, J. L., Counterion-Dependent Excitonic Spectra of Tetra(*p*-carboxyphenyl)porphyrin Aggregates in Acidic Aqueous Solution. *J. Am. Chem. Soc.* **2003,** *125*, 810-820.

(25) De Luca, G.; Romeo, A.; Scolaro, L. M., Counteranion Dependent Protonation and Aggregation of Tetrakis(4-sulfonatophenyl)porphyrin in Organic Solvents. *J. Phys. Chem. B* **2006,** *110*, 7309-7315.

(26) Nakata, K.; Kobayashi, T.; Tokunaga, E., Electric Field-Controlled Dissociation and Association of Porphyrin J-aggregates in Aqueous Solution. *Phys. Chem. Chem. Phys.* **2011,** *13*, 17756-17767.

(27) Castriciano, M. A.; Romeo, A.; Villari, V.; Angelini, N.; Micali, N.; Scolaro, L. M., Aggregation Behavior of Tetrakis(4-sulfonatophenyl)porphyrin in AOT/Water/Decane Microemulsions. *J. Phys. Chem. B* **2005,** *109*, 12086-12092.

(28) Castriciano, M. A.; Romeo, A.; Villari, V.; Micali, N.; Scolaro, L. M., Nanosized Porphyrin J-aggregates in Water/AOT/Decane Microemulsions. *J. Phys. Chem. B* **2004,** *108*, 9054-9059.

(29) Fujiwara, K.; Wada, S.; Monjushiro, H.; Watarai, H., Ion-Association Aggregation of an Anionic Porphyrin at the Liquid/Liquid Interface Studied by Second Harmonic Generation Spectroscopy. *Langmuir* **2006,** *22*, 2482-2486.

(30) Fujiwara, K.; Monjushiro, H.; Watarai, H., Non-Linear Optical Activity of Porphyrin Aggregate at the Liquid/Liquid Interface. *Chem. Phys. Lett.* **2004,** *394*, 349-353.

(31) Okumura, R.; Hinoue, T.; Watarai, H., Ion-Association Adsorption of Water-Soluble Porphyrin at a Liquid-Liquid Interface and an External Electric Field Effect on the Adsorption. *Anal. Sci.* **1996,** *12*, 393-397.

(32) Smith, K. M., *Porphyrins and Metalloporphyrins*. Elsevier Amsterdam: 1975.

(33) Bhosale, S. V.; Shitre, G. V.; Bobe, S. R.; Gupta, A., Supramolecular Chemistry of Protoporphyrin IX and its Derivatives. *Eur. J. Org. Chem.* **2013**, 3939-3954.

(34) Ethirajan, M.; Chen, Y.; Joshi, P.; Pandey, R. K., The Role of Porphyrin Chemistry in Tumor Imaging and Photodynamic Therapy. *Chem. Soc. Rev.* **2011,** *40*, 340-362.

(35) Castano, A. P.; Demidova, T. N.; Hamblin, M. R., Mechanisms in Photodynamic Therapy: Part One - Photosensitizers, Photochemistry and Cellular Localization. *Photodiagn. Photodyn. Ther.* **2004,** *1*, 279-293.

(36) Delmarre, D.; Meallet-Renault, R.; Bied-Charreton, C.; Pasternack, R. F., Incorporation of Water-Soluble Porphyrins in Sol-Gel Matrices and Application to pH Sensing. *Anal. Chim. Acta* **1999,** *401*, 125-128.

(37) Chen, J.; Collier, C. P., Noncovalent Functionalization of Single-Walled Carbon Nanotubes with Water-Soluble Porphyrins. *J. Phys. Chem. B* **2005,** *109*, 7605-7609.

(38) Fermín, D. J.; Duong, H. D.; Ding, Z.; Brevet, P. F.; Girault, H. H., Photoinduced Electron Transfer at Liquid/Liquid Interfaces. Part II. A Study of the Electron Transfer and

Recombination Dynamics by Intensity Modulated Photocurrent Spectroscopy (IMPS). *Phys. Chem. Chem. Phys.* **1999,** *1*, 1461-1467.

(39) Wandlowski, T.; Marecek, V.; Samec, Z., Galvani Potential Scales for Water-Nitrobenzene and Water-1,2-Dichloroethane Interfaces. *Electrochim. Acta* **1990,** *35*, 1173-1175.

(40) Nagatani, H.; Samec, Z.; Brevet, P. F.; Fermín, D. J.; Girault, H. H., Adsorption and Aggregation of *meso*-Tetrakis(4-carboxyphenyl)porphyrinato Zinc(II) at the Polarized Water|1,2-Dichloroethane Interface. *J. Phys. Chem. B* **2003,** *107*, 786-790.

(41) Langevin, D., *Light Scattering by Liquid Surfaces and Complementary Techniques*. Marcel Dekker: New York, 1992; p 89-104.

(42) Osakai, T.; Muto, K., Ion Transfer and Photoinduced Electron Transfer of Water-Soluble Porphyrin at the Nitrobenzene|Water Interface. *J. Electroanal. Chem.* **2001,** *496*, 95-102.

(43) Gouterman, M., Spectra of Porphyrins. *J. Mol. Spectrosc.* **1961,** *6*, 138-163.

(44) Improta, R.; Ferrante, C.; Bozio, R.; Barone, V., The Polarizability in Solution of Tetra-Phenyl-Porphyrin Derivatives in their Excited Electronic States: A PCM/TD-DFT Study. *Phys. Chem. Chem. Phys.* **2009,** *11*, 4664-4673.

(45) Chen, D. M.; He, T.; Cong, D. F.; Zhang, Y. H.; Liu, F. C., Resonance Raman Spectra and Excited-State Structure of Aggregated Tetrakis(4-sulfonatophenyl)porphyrin Diacid. *J. Phys. Chem. A* **2001,** *105*, 3981-3988.

(46) Rubires, R.; Farrera, J. A.; Ribó, J. M., Stirring Effects on the Spontaneous Formation of Chirality in the Homoassociation of Diprotonated *meso*-Tetraphenylsulfonato Porphyrins. *Chem. Eur. J.* **2001,** *7*, 436-446.

(47) Ribo, J. M.; Crusats, J.; Farrera, J.-A.; Valero, M. L., Aggregation in Water Solutions of Tetrasodium Diprotonated *meso*-Tetrakis(4-sulfonatophenyl)porphyrin. *J. Chem. Soc., Chem. Commun.* **1994**, 681-682.

(48) Maiti, N. C.; Ravikanth, M.; Mazumdar, S.; Periasamy, N., Fluorescence Dynamics of Noncovalently Linked Porphyrin Dimers, and Aggregates. *J. Phys. Chem.* **1995,** *99*, 17192-17197.

(49) Maiti, N. C.; Mazumdar, S.; Periasamy, N., J- and H-Aggregates of Porphyrin-Surfactant Complexes: Time-Resolved Fluorescence and Other Spectroscopic Studies. *J. Phys. Chem. B* **1998,** *102*, 1528-1538.

(50) Miyata, A.; Unuma, Y.; Higashigaki, Y., H-Aggregate of a Long-Chain Crystal Violet Dye in Langmuir-Blodgett Films. *Bull. Chem. Soc. Jpn.* **1991,** *64*, 2786-2791.

(51) Watarai, H.; Wada, S.; Fujiwara, K., Spectroscopic Detection of Chiral Aggregation at Liquid-Liquid Interfaces. *Tsinghua Sci. Technol.* **2006,** *11*, 228-232.

(52) Perrenoud-Rinuy, J.; Brevet, P.-F.; Girault, H. H., Second Harmonic Generation Study of Myoglobin and Hemoglobin and their Protoporphyrin IX Chromophore at the Water/1,2-Dichloroethane Interface. *Phys. Chem. Chem. Phys.* **2002,** *4*, 4774-4781.

(53) Margalit, R.; Shaklai, N.; Cohen, S., Fluorimetric Studies on the Dimerization Equilibrium of Protoporphyrin IX and its Haemato Derivative. *Biochem. J* **1983,** *209*, 547-552.

(54) Bobe, M. S. R.; Al Kobaisi, M.; Bhosale, S. V., Solvent-Tuned Self-Assembled Nanostructures of Chiral L/D-Phenylalanine Derivatives of Protoporphyrin IX. *ChemistryOpen* **2015,** *4*, 516-522.

(55) Monsu Scolaro, L.; Castriciano, M.; Romeo, A.; Patane, S.; Cefali, E.; Allegrini, M., Aggregation Behavior of Protoporphyrin IX in Aqueous Solutions: Clear Evidence of Vesicle Formation. *J. Phys. Chem. B* **2002,** *106*, 2453-2459.

(56) Brault, D., Physical Chemistry of Porphyrins and Their Interactions with Membranes: The Importance of pH. *J. Photochem. Photobiol., B* **1990,** *6*, 79-86.

(57) Inamura, I.; Uchida, K., Association Behavior of Protoporphyrin IX in Water and Aqueous Poly(*N*-vinylpyrrolidone) Solutions. Interaction between Protoporphyrin IX and Poly(*N*-vinylpyrrolidone). *Bull. Chem. Soc. Jpn.* **1991,** *64*, 2005-2007.

(58) Walker, R. A.; Conboy, J. C.; Richmond, G. L., Molecular Structure and Ordering of Phospholipids at a Liquid-Liquid Interface. *Langmuir* **1997,** *13*, 3070-3073.

(59) Santos, H. A.; García-Morales, V.; Pereira, C. M., Electrochemical Properties of Phospholipid Monolayers at Liquid-Liquid Interfaces. *ChemPhysChem* **2010,** *11*, 28-41.

(60) Pichot, R.; Watson, R. L.; Norton, I. T., Phospholipids at the Interface: Current trends and Challenges. *Int. J. Mol. Sci.* **2013,** *14*, 11767-11794.

(61) Samec, Z.; Trojanek, A.; Girault, H. H., Thermodynamic Analysis of the Cation Binding to a Phosphatidylcholine Monolayer at a Polarised Interface between Two Immiscible Electrolyte Solutions. *Electrochem. Commun.* **2003,** *5*, 98-103.

(62) Yoshida, Y.; Maeda, K.; Shirai, O., The Complex Formation of Ions with a Phospholipid Monolayer Adsorbed at an Aqueous|1,2-Dichloroethane Interface. *J. Electroanal. Chem.* **2005,** *578*, 17-24.

## TOC GRAPHICS